Available online at www.sciencedirect.com
ScienceDirect
Journal of Sound and Vibration 306 (2007) 946–954
JOURNAL OF SOUND AND VIBRATION
www.elsevier.com/locate/jsvi

Short Communication

Torsional vibration analyses of a damped shafting system using tapered shaft element

Jia-Jang Wu*

Department of Marine Engineering, National Kaohsiung Marine University, No. 142, Hai-Chuan Road, Nan-Tzu, Kaohsiung 811, Taiwan, Republic of China

Received 30 May 2007; accepted 31 May 2007
Available online 20 July 2007

Abstract

The objective of this paper is to present a *tapered shaft element* such that the torsional vibration characteristics of a damped shafting system can be easily determined with effect of continuous non-uniformity of the shaft cross-sections being considered. To this end, the shape functions of the tapered shaft element are firstly derived. Then, the stiffness and mass matrices of the last shaft element are determined by means of the Lagrange's equations. To confirm the reliability of the presented theory, the numerical results obtained from the presented technique are compared with those obtained from the existing literature and good agreement is achieved. Finally, the torsional vibration analysis of a hybrid (tapered) shaft, composed of multiple uniform and tapered shaft segments and carrying multiple disks, is performed to show the applicability of the presented technique.

1. Introduction

Torsional vibration characteristics are important information for shafting system designers. Thus, many researchers have studied the relating problems. For example, Chen [1] has investigated the torsional vibrations of a cylinder with varying cross-section and adhesive masses. Aleyaasin et al. [2] have used the transfer matrix method to perform the flexural vibration analysis of a rotor mounted on fluid film bearings. Koser and Pasin [3] have studied the torsional vibrations of the drive shafts and mechanisms by means of analytical approach. Wu and Chen [4] have presented a technique to replace a gear-branched system with an equivalent straight-geared system and then used the last model incorporated with the finite element method to study the torsional vibration characteristics of the gear-branched system. Khulief and Mohiuddin [5] have investigated the torsional dynamic behaviour of a rotor-bearing system using finite element method and modal reduction technique. Qing and Cheng [6] have studied the coupled torsional and lateral vibrations of rotor-shaft systems using finite element method. Nelson and Mcvaugh [7] and Zorzi and Nelson [8] have performed the lateral vibration analyses of a rotor-bearing system. Wu and Yang [9], Al-Bedoor [10] and Mohiuddin and Khulief

*Tel.: +886 78100888x5230; fax: +886 62808458.
E-mail address: jjangwu@mail.nkmu.edu.tw

0022-460X/$ - see front matter © 2007 Elsevier Ltd. All rights reserved.
doi:10.1016/j.jsv.2007.05.050

[11] have investigated the torsional and lateral vibration of shafting system with transfer matrix method and Lagrangian dynamics method.

From review of the foregoing existing literature, one finds that only Refs. [1,11] have considered the effect of continuous non-uniformity of shaft cross-sections. In Ref. [1], the formulations were developed based on the analytical method, thus, they cannot be easily used to perform the torsional vibration analysis of a damped hybrid (tapered) shaft, composed of multiple uniform and tapered shaft segments and carrying multiple disks (cf. Fig. 5). In Ref. [11], the shape functions for the conventional *uniform* shaft element are used to derive the stiffness and mass matrices of a conical shaft element. To improve the drawbacks of some existing literature concerned, this paper presents the theory concerning a *tapered shaft element*, so that the torsional vibration characteristics of a damped shafting system can be easily obtained with continuous non-uniformity of the shaft cross-sections being considered. In which, the shape functions of the *tapered shaft element* are firstly derived and then its stiffness and mass matrices are determined by means of the Lagrange's equations. For validation, the numerical results obtained from the presented technique are compared with the existing literature and good agreement is achieved.

2. Shape functions of a tapered shaft element

Fig. 1 shows an arbitrary tapered shaft element. In which, ⓘ and ⓚ are respectively the numberings for the two nodes of the shaft element, T_i, θ_i and d_i denote the external torque, twist angle and shaft diameter at node ⓘ, respectively, while T_k, θ_k and d_k denote the corresponding ones at node ⓚ, respectively. Besides, ℓ is total length of the tapered shaft element and G is shear modulus of the shaft material. For the tapered shaft element shown in Fig. 1, the twist angle $\theta(x)$ of the cross-section at position x is given by

$$\theta(x) = \theta_i + \phi(x), \tag{1}$$

where $\phi(x)$ is the relative twist angle between the cross-section at position x and that at node ⓘ. It is given by [12]

$$\phi(x) = \int_0^x \frac{(T_k - T_i)}{GI(\tilde{x})}\,\mathrm{d}\tilde{x} = \frac{(T_k - T_i)}{G}\int_0^x \frac{1}{I(\tilde{x})}\,\mathrm{d}\tilde{x}. \tag{2}$$

In Eq. (2), $I(\tilde{x})$ represents the polar moment of inertia of the cross-sectional area about x-axis for the cross-section at position $\tilde{x}$ given by

$$I(\tilde{x}) = I_0\left[1 + \alpha\left(\frac{\tilde{x}}{\ell}\right)\right]^4, \quad I_0 = \frac{\pi d_i^4}{32}, \quad \alpha = \frac{d_k - d_i}{d_i}. \tag{3}$$

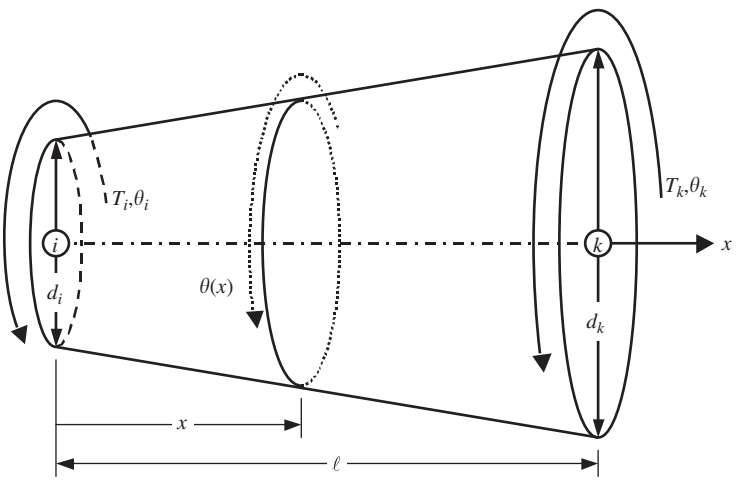

Fig. 1. Mathematical model of a tapered shaft element.

From Eq. (1), one has the twist angle at position $x = \ell$ to be $\theta(\ell) = \theta_i + \phi(\ell) = \theta_k$, thus,

$$\frac{\theta_k - \theta_i}{\phi(\ell)} = 1. \tag{4}$$

Introducing Eq. (4) into Eq. (1) leads to

$$\theta(x) = \theta_i + \frac{\phi(x)}{\phi(\ell)}(\theta_k - \theta_i) = N_i(x)\theta_i + N_k(x)\theta_k. \tag{5}$$

The values of $\phi(x)$ and $\phi(\ell)$ appearing in the last equation are determined by Eqs. (2) and (3), and substituting them into Eq. (5) yields:

$$N_i(x) = 1 - \zeta, \quad N_k(x) = \zeta, \tag{6}$$

with

$$\zeta = \frac{\phi(x)}{\phi(\ell)} = \frac{d_k^3[(d_i x - d_k x)^2 + 3d_i\ell(d_i\ell - d_i x + d_k x)]x}{(d_k^2 + d_i d_k + d_i^2)(d_i\ell - d_i x + d_k x)^3}. \tag{7}$$

According to definition, $N_i(x)$ and $N_k(x)$ appearing in Eq. (5) and respectively defined by Eqs. (6) and (7) represent the shape functions of the tapered shaft element shown in Fig. 1.

3. Stiffness and mass matrices of the tapered shaft element

In this section, the stiffness and mass matrices of the tapered shaft element are derived from the following Lagrange's equations [13]:

$$\frac{\partial}{\partial t}\left(\frac{\partial U}{\partial \dot{\theta}_\lambda}\right) - \frac{\partial U}{\partial \theta_\lambda} + \frac{\partial V}{\partial \theta_\lambda} = T_\lambda \quad (\lambda = i, k), \tag{8}$$

where U is kinetic energy and V is strain energy of the tapered shaft element (cf. Fig. 1) given by

$$U = \frac{1}{2}\int_0^\ell \rho I(x)\dot{\theta}^2(x)\,\mathrm{d}x, \quad V = \frac{1}{2}\int_0^\ell GI(x)\theta'^2(x)\,\mathrm{d}x, \tag{9}$$

where the overhead dot $(\cdot)$ and the prime $(')$ represent differentiations with respect to time t and axial coordinate x, respectively.

Substituting Eq. (5) into Eq. (9), and then introducing the resulting expressions for U and V into Eq. (8), one obtains

$$\left[\rho\int_0^\ell I(x)N_i^2(x)\,\mathrm{d}x\right]\ddot{\theta}_i + \left[\rho\int_0^\ell I(x)N_i(x)N_k(x)\,\mathrm{d}x\right]\ddot{\theta}_k + \left[G\int_0^\ell I(x)N_i'^2(x)\,\mathrm{d}x\right]\theta_i + \left[G\int_0^\ell I(x)N_i'(x)N_k'(x)\,\mathrm{d}x\right]\theta_k = T_i, \tag{10}$$

$$\left[\rho\int_0^\ell I(x)N_i(x)N_k(x)\,\mathrm{d}x\right]\ddot{\theta}_i + \left[\rho\int_0^\ell I(x)N_k^2(x)\,\mathrm{d}x\right]\ddot{\theta}_k + \left[G\int_0^\ell I(x)N_i'(x)N_k'(x)\,\mathrm{d}x\right]\theta_i + \left[G\int_0^\ell I(x)N_k'^2(x)\,\mathrm{d}x\right]\theta_k = T_k. \tag{11}$$

Substituting Eqs. (3) and (6) into Eqs. (10) and (11) gives

$$[m]\{\ddot{\theta}\} + [k]\{\theta\} = \{T\}, \tag{12}$$

where

$$\{\ddot{\theta}\} = [\,\ddot{\theta}_i \quad \ddot{\theta}_k\,]^{\mathrm{T}}, \quad \{\theta\} = [\theta_i, \theta_k]^{\mathrm{T}}, \quad \{T\} = [\,T_i \quad T_k\,]^{\mathrm{T}}, \tag{13}$$

$$[k] = \frac{3G\pi d_i^3 d_k^3}{32\ell(d_i^2 + d_i d_k + d_k^2)} \begin{bmatrix} 1 & -1 \\ -1 & 1 \end{bmatrix}, \tag{14}$$

$$[m] = \frac{\rho\ell\pi}{320(d_i^2 + d_i d_k + d_k^2)^2} \begin{bmatrix} A_{11} & A_{12} \\ A_{21} & A_{22} \end{bmatrix}, \tag{15}$$

$$A_{11} = 2d_i^5(d_i^3 + 6d_i d_k^2 + 3d_i^2 d_k + 5d_k^3), \quad A_{12} = A_{21} = 3d_i^3 d_k^3(d_i^2 + 3d_i d_k + d_k^2),$$
$$A_{22} = 2d_k^5(5d_i^3 + 3d_i d_k^2 + 6d_i^2 d_k + d_k^3), \tag{16}$$

Eqs. (14) and (15), respectively represent the stiffness and mass matrices of the tapered shaft element.

4. Torsional vibration analyses of the damped tapered shafting system

4.1. Equations of motion of the damped tapered shafting system

For free vibration of a damped multiple degree-of-freedom (dof) shafting system (cf. Figs. 4 and 5), its equations of motion take the form:

$$[\bar{M}^*]\{\ddot{\bar{\theta}}\} + [\bar{C}^*]\{\dot{\bar{\theta}}\} + [\bar{K}^*]\{\bar{\theta}\} = \{0\}, \tag{17}$$

where $\{\ddot{\bar{\theta}}\}$, $\{\dot{\bar{\theta}}\}$ and $\{\bar{\theta}\}$, respectively, represent the angular acceleration, velocity and displacement vectors, while $[\bar{M}^*]$, $[\bar{C}^*]$ and $[\bar{K}^*]$, respectively, represent the overall mass, damping and stiffness matrices of the entire shafting system given by

$$[\bar{M}^*] = [\bar{M}] + [J], \quad [\bar{K}^*] = [\bar{K}], \quad [\bar{C}^*] = [\bar{C}] + [C], \tag{18}$$

where

$$\bar{M}^*_{ij} = \bar{M}_{ij}, \quad \bar{K}^*_{ij} = \bar{K}_{ij}, \quad \bar{C}^*_{ij} = \bar{C}_{ij} \quad (i = 1 \text{ to } n;\ j = 1 \text{ to } n), \tag{19}$$

except

$$\bar{M}^*_{s_i s_i} = \bar{M}_{s_i s_i} + J_i \quad (i = 1 \text{ to } n_d), \quad \bar{C}^*_{s_j s_j} = \bar{C}_{s_j s_j} + c_j \quad (j = 1 \text{ to } n_c). \tag{20}$$

In the last expressions, $[\bar{M}]$, $[\bar{C}]$ and $[\bar{K}]$, respectively, represent the overall mass, damping and stiffness matrices of the *bare* tapered shaft itself (i.e., the shaft *without any disk and rotational damper* attached), n_d and n_c, respectively represent the total number of the disks and rotational dampers attached to the shafting system; n represents the total dofs of the entire shafting system; J_i and c_j, respectively represent the mass moment of inertia of the ith disk and damping coefficient of the jth rotational damper, while the subscript s_i and s_j represent the numberings for the dofs of the ith disk and jth rotational damper, respectively.

4.2. Eigenvalues and eigenvectors of the damped tapered shafting system

In order to determine the free vibration characteristics of the damped shafting system, the original $n \times n$ equations of motion, Eq. (17), are transformed into the $2n \times 2n$ ones [14,15]:

$$[\tilde{M}]\{\dot{\tilde{\theta}}\} + [\tilde{K}]\{\tilde{\theta}\} = \{0\}, \tag{21}$$

where

$$[\tilde{M}] = \begin{bmatrix} [0]_{n\times n} & [\bar{M}^*]_{n\times n} \\ [\bar{M}^*]_{n\times n} & [\bar{C}^*]_{n\times n} \end{bmatrix}_{2n\times 2n}, \quad [\tilde{K}] = \begin{bmatrix} -[\bar{M}^*]_{n\times n} & [0]_{n\times n} \\ [0]_{n\times n} & [\bar{K}^*]_{n\times n} \end{bmatrix}_{2n\times 2n} \tag{22}$$

$$\{\tilde{\theta}\} = [\,\{\dot{\bar{\theta}}\} \quad \{\bar{\theta}\}\,]^{\mathrm{T}}_{1\times 2n}, \quad \{\dot{\tilde{\theta}}\} = [\,\{\ddot{\bar{\theta}}\} \quad \{\dot{\bar{\theta}}\}\,]^{\mathrm{T}}_{1\times 2n}, \tag{23}$$

For free vibration, the vector $\{\tilde{\theta}\}$ takes the form:

$$\{\tilde{\theta}\} = \{\Phi\}\, e^{\Omega t}, \tag{24}$$

where $\{\Phi\}$ is the eigenvector (or the amplitude of $\{\tilde{\theta}\}$), Ω is the eigenvalue and t is time.

The substitution of Eq. (24) into Eq. (21) leads to

$$([\tilde{K}] + \Omega_i[\tilde{M}])\{\Phi\}_i = \{0\} \quad (i = 1 \text{ to } 2n). \tag{25}$$

Eq. (25) is a standard eigenvalue problem and can be solved using the subroutine EISPACK [16].

5. Property matrices of a uniform shaft element

Since a *uniform* shaft is the special case of a *tapered* shaft, one of the reasonable ways for confirming the reliability of the presented approach is to compare the natural frequencies of a tapered shafting system with the corresponding ones of a uniform one. The stiffness and mass matrices of the uniform shaft element are given by [17]:

$$[k] = \frac{G\pi d_s^4}{32\ell}\begin{bmatrix} 1 & -1 \\ -1 & 1 \end{bmatrix}, \quad [m] = \frac{\rho\ell\pi d_s^4}{32}\begin{bmatrix} \frac{1}{3} & \frac{1}{6} \\ \frac{1}{6} & \frac{1}{3} \end{bmatrix}, \tag{26}$$

where d_s is the diameter for cross-sections of the uniform shaft element.

6. Numerical results and discussions

6.1. Reliability of presented theory and developed computer program

Fig. 2(a) shows an undamped *uniform* clamped-free shaft carrying a disk at its free end. For convenience, the last system is called *U-shaft* here. The physical properties for the *U-shaft* are: shear modulus $G = 8.01 \times 10^{10}\,N/m^2$, mass density $\rho_s = 7820\,kg/m^3$, shaft diameter $d_s = 0.041\,m$, total shaft length $\ell_s = 1.8\,m$, and mass moment of inertia of disk $J = 3.904 \times 10^{-3}\,kg\,m^2$. All the physical properties for the *tapered* shafting system shown in Fig. 2(b) are exactly the same as those for the *U-shaft* except that the diameters of the cross-sections at the *left* end and *right* end of the tapered shaft are d_ℓ and d_r, respectively. For convenience, the last shafting system is called *T-shaft* here. It is obvious that the eigenvalues of *T-shaft* will be close to those of *U-shaft* if the total length and total mass of *T-shaft* are exactly the same as those of *U-shaft*, and the average value of both d_ℓ and d_r is close to that of d_s. In other words, the smaller the value of $|d_\ell - d_r|$, the smaller the differences between the eigenvalues of *T-shaft* and *U-shaft*. Five sets of d_ℓ and d_r are investigated in this subsection: (a) $d_\ell = d_r = 0.041\,m$, (b) $d_\ell = 0.042\,m$ and $d_r = 0.03999\,m$, (c) $d_\ell = 0.043\,m$ and $d_r = 0.03898\,m$, (d) $d_\ell = 0.044\,m$ and $d_r = 0.03792\,m$ and (e) $d_\ell = 0.045\,m$ and $d_r = 0.03686\,m$. Note that the last five sets of diameters for the *T-shaft* are determined based on the assumption that the total length and

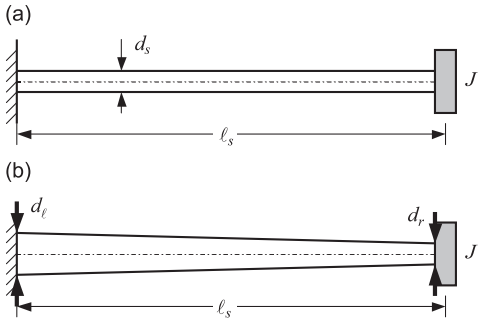

Fig. 2. A clamped-free shaft carrying a disk at its free end: (a) *uniform* shaft (*U-shaft*) and (b) *tapered* shaft (*T-shaft*).

Table 1
The first five eigenvalues, $\bar{\omega}_j = \bar{\omega}_{jR} \pm \bar{i}\bar{\omega}_{jI}$ ($j = 1$ to 5), of a clamped-free *T-shaft* and a clamped-free *U-shaft*

Methods	Diameters (m)		Eigenvalues, $\bar{\omega}_j = \bar{\omega}_{jR} \pm \bar{i}\bar{\omega}_{jI}$ ($j = 1$ to 5) (rad/s)				
	d_ℓ	d_r	$\bar{\omega}_1$	$\bar{\omega}_2$	$\bar{\omega}_3$	$\bar{\omega}_4$	$\bar{\omega}_5$
Tapered shaft element (*T-shaft*)	0.045	0.03686	−3.49E−8±*1573.39* $\bar{i}$	5.30E−7±*5957.49* $\bar{i}$	−7.41E−7±*11370.22* $\bar{i}$	1.06E−6±*16904.89* $\bar{i}$	8.95E−7±*22482.24* $\bar{i}$
	0.044	0.03792	−6.08E−8±*1569.11* $\bar{i}$	−1.22E−6±*5985.84* $\bar{i}$	−6.84E−7±*11386.53* $\bar{i}$	3.60E−7±*16916.08* $\bar{i}$	2.44E−7±*22490.71* $\bar{i}$
	0.043	0.03898	1.98E−7±*1560.61* $\bar{i}$	3.70E−7±*6018.53* $\bar{i}$	9.76E−7±*11405.86* $\bar{i}$	−1.23E−7±*16929.44* $\bar{i}$	1.15E−6±*22500.87* $\bar{i}$
	0.042	0.03999	6.48E−7±*1547.02* $\bar{i}$	2.07E−6±*6053.29* $\bar{i}$	−3.16E−7±*11427.06* $\bar{i}$	2.41E−7±*16944.13* $\bar{i}$	−8.84E−7±*22512.12* $\bar{i}$
	0.041	0.041	2.20E−7±*1529.83* $\bar{i}$	1.5E−6±*6091.67* $\bar{i}$	6.03E−7±*11451.04* $\bar{i}$	9.62E−7±*16960.96* $\bar{i}$	1.20E−6±*22524.89* $\bar{i}$
Uniform shaft element (*U-shaft*)	0.041	0.041	2.20E−7±*1529.83* $\bar{i}$	1.5E−6±*6091.67* $\bar{i}$	6.03E−7±*11451.04* $\bar{i}$	9.62E−7±*16960.96* $\bar{i}$	1.20E−6±*22524.89* $\bar{i}$
Analytical method [15]	0.041	0.041	1529.74	6090.81	11445.82	16943.64	22483.79

Table 2
The first five eigenvalues, $\bar{\omega}_j = \bar{\omega}_{jR} \pm \bar{i}\bar{\omega}_{jI}$ ($j = 1$ to 5), of a free–free tapered shaft

Methods	Diameters (m)		Eigenvalues, $\bar{\omega}_j = \bar{\omega}_{jR} \pm \bar{i}\bar{\omega}_{jI}$ ($j = 1$ to 5) (rad/s)				
	d_ℓ	d_r	$\bar{\omega}_1$	$\bar{\omega}_2$	$\bar{\omega}_3$	$\bar{\omega}_4$	$\bar{\omega}_5$
Tapered shaft element	0.041	0.05125	1.12E−6±*5670.15* $\bar{i}$	6.47E−7±*11219.16* $\bar{i}$	−2.64E−6±*16803.15* $\bar{i}$	−1.39E−6±*22405.64* $\bar{i}$	5.01E−7±*28026.28* $\bar{i}$
Ref. [1]			5666.77	11208.49	16777.57	22353.34	27932.46
Ref. [11]			5670.14	11219.15	16803.12	22405.57	28026.19

total mass of *T-shaft* are exactly the same as those of *U-shaft*. Table 1 shows the first five eigenvalues, $\bar{\omega}_j = \bar{\omega}_{jR} \pm \bar{i}\bar{\omega}_{jI}$ ($j = 1$ to 5), for *U-* and *T-shaft*. From the table, one sees that the imaginary parts of the eigenvalues, $\bar{\omega}_{jI}$, of *T-shaft* and *U-shaft* with $d_\ell = d_r = 0.041\,\text{m} = d_s$ are very close to the corresponding ones obtained from the analytical method. Besides, the smaller the value of $|d_\ell - d_r|$, the smaller the differences between the imaginary parts of the eigenvalues, $\bar{\omega}_{jI}$, of *T-shaft* and *U-shaft*. Moreover, the real parts of the eigenvalues, $\bar{\omega}_{jR}$, for the last two systems are very small and negligible due to the fact that $[\bar{C}^*] = [0]$. In view of the last reasonable results, it is believed that the presented theory regarding *tapered shaft element* should be reliable.

In addition, a free–free tapered shaft with diameters of cross-sections at its left end $d_\ell = 0.041\,\text{m}$ and right end $d_r = 0.041(1 + 0.25) = 0.05125\,\text{m}$ is also studied here. The total length, shear modulus and mass density of the free–free tapered shaft are exactly the same as those of the foregoing clamped-free *T-shaft*. Table 2 shows the first five eigenvalues, $\bar{\omega}_j = \bar{\omega}_{jR} \pm \bar{i}\bar{\omega}_{jI}$ ($j = 1$ to 5), of the free–free tapered shaft. It is seen that the imaginary parts of the eigenvalues, $\bar{\omega}_{jI}$, obtained from the presented *tapered shaft element* are very close to the corresponding ones obtained from Refs. [1] and [11]. The last results further confirm the reliability of the presented *tapered shaft element*.

6.2. Influence of non-uniformity of the shaft cross-sections

The shafting system investigated here is an undamped free–free tapered shaft carrying a disk at its mid-length, as shown in Fig. 3. The physical properties of the shafting system are: total shaft length $\ell_s = 2.4\,\text{m}$, diameter of left end $d_\ell = 0.041 - 0.045\,\text{m}$, diameter of right end $d_r = 0.04497 - 0.04096\,\text{m}$ (cf. Table 3) and mass moment of inertia of the disk $J = 4.583 \times 10^{-3}\,\text{kg m}^2$. The shear modulus and mass density of the current tapered shaft are exactly the same as those of the *T-shaft* (or *U-shaft*) studied in the last subsection. The torsional vibration analyses with five sets of diameters, d_ℓ and d_r, are conducted (cf. Table 3): (a) $d_\ell = 0.041\,\text{m}$ and $d_r = 0.04497\,\text{m}$, (b) $d_\ell = 0.042\,\text{m}$ and $d_r = 0.04399\,\text{m}$, (c) $d_\ell = d_r = 0.043\,\text{m}$, (d) $d_\ell = 0.044\,\text{m}$ and

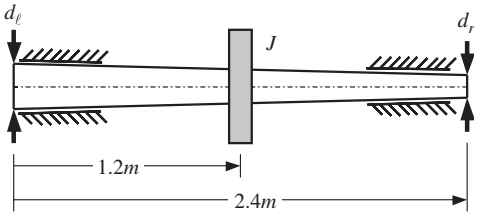

Fig. 3. An undamped free–free tapered shaft carrying a disk at its mid-length.

Table 3
The first five eigenvalues, $\bar{\omega}_j = \bar{\omega}_{jR} \pm \bar{i}\bar{\omega}_{jI}$ ($j = 1$ to 5), of a free–free tapered shaft carrying a disk at its mid-length, as shown in Fig. 3

Diameters (m)		Eigenvalues, $\bar{\omega}_j = \bar{\omega}_{jR} \pm \bar{i}\bar{\omega}_{jI}$ ($j = 1$ to 5) (rad/s)				
d_ℓ	d_r	$\bar{\omega}_1$	$\bar{\omega}_2$	$\bar{\omega}_3$	$\bar{\omega}_4$	$\bar{\omega}_5$
0.041	0.04497	7.41E−7±*4189.94* $\bar{i}$	1.68E−6±*5698.64* $\bar{i}$	1.63E−7±*12581.13* $\bar{i}$	9.73E−7±*13289.91* $\bar{i}$	−1.66E−7±*21006.86* $\bar{i}$
0.042	0.04399	5.64E−7±*4189.96* $\bar{i}$	1.85E−7±*5714.73* $\bar{i}$	7.94E−8±*12581.14* $\bar{i}$	7.93E−8±*13301.26* $\bar{i}$	5.56E−7±*21006.88* $\bar{i}$
0.043	0.04300	2.06E−7±*4189.87* $\bar{i}$	1.24E−6±*5712.06* $\bar{i}$	5.03E−7±*12581.12* $\bar{i}$	−3.05E−7±*13299.95* $\bar{i}$	−8.22E−8±*21006.85* $\bar{i}$
0.044	0.04199	9.13E−7±*4189.96* $\bar{i}$	1.45E−7±*5714.79* $\bar{i}$	4.62E−7±*12581.14* $\bar{i}$	4.69E−7±*13301.29* $\bar{i}$	9.39E−7±*21006.84* $\bar{i}$
0.045	0.04096	−4.39E−7±*4190.19* $\bar{i}$	−8.11E−8±*5723.16* $\bar{i}$	−1.05E−8±*12581.22* $\bar{i}$	−3.59E−7±*13305.38* $\bar{i}$	8.35E−7±*21006.90* $\bar{i}$

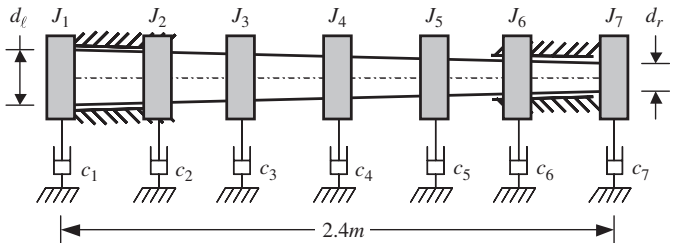

Fig. 4. A damped tapered shaft carrying seven equally spaced identical disks.

$d_r = 0.04199$ m and (e) $d_\ell = 0.045$ m and $d_r = 0.04096$ m. The last five sets of diameters are determined based on the assumption that the total length and total mass of the tapered shaft remain unchanged. Table 3 shows the first five eigenvalues, $\bar{\omega}_j = \bar{\omega}_{jR} \pm \bar{i}\bar{\omega}_{jI}$ ($j = 1$ to 5), of the shafting system shown in Fig. 3. From the table, one sees that the small variation of the cross-sections of the tapered shaft will influence the eigenvalues, $\bar{\omega}_j = \bar{\omega}_{jR} \pm \bar{i}\bar{\omega}_{jI}$, of the entire shafting system to some degree even if the total length and total mass of the tapered shaft remain unchanged.

6.3. Influence of damping coefficient

Fig. 4 shows a free–free tapered shaft carrying seven equally spaced identical disks. The physical properties of the tapered shaft are exactly the same as those of the example studied in the last subsection except that the diameters of the left end and right end are $d_\ell = 0.044$ m and $d_r = 0.04199$ m, respectively. Besides, the mass moment of inertia of each disk is identical and given by $J_i = 2.427 \times 10^{-2}/7\,\mathrm{kg\,m^2}$ ($i = 1$–7). Furthermore, the damping coefficients c_i ($i = 1$–7) are taken to be 2.73, 5.46 or 8.19 N s/m (cf. Table 4).

Table 4 shows the influence of damping coefficients, c_i ($i = 1$–7), on the first five eigenvalues of the shafting system, $\bar{\omega}_j = \bar{\omega}_{jR} \pm \bar{i}\bar{\omega}_{jI}$ ($j = 1$ to 5). For comparison, the first five eigenvalues of the shafting system with damping effects neglected (i.e., $c_i = 0$) are also shown in the final row of Table 4. From the 3rd row to the 5th row of the table, one sees that the influence of damping coefficients c_i on the natural frequencies, $\bar{\omega}_{jI}$, is much

Table 4
The first five eigenvalues, $\bar{\omega}_j = \bar{\omega}_{jR} \pm \bar{i}\bar{\omega}_{jI}$ ($j = 1$ to 5), of a damped free–free tapered shaft carrying seven equally spaced identical disks, as shown in Fig. 4

Damping coefficients, c_d (N s/m)	Eigenvalues, $\bar{\omega}_j = \bar{\omega}_{jR} \pm \bar{i}\bar{\omega}_{jI}$ ($j = 1$ to 5) (rad/s)				
	$\bar{\omega}_1$	$\bar{\omega}_2$	$\bar{\omega}_3$	$\bar{\omega}_4$	$\bar{\omega}_5$
2.73	−3.24E2±*1748.48* $\bar{i}$	−3.29E2±*3474.72* $\bar{i}$	−3.53E2±*5053.05* $\bar{i}$	−3.43E2±*6410.28* $\bar{i}$	−3.50E2±*7461.85* $\bar{i}$
5.46	−6.49E2±*1655.93* $\bar{i}$	−6.58E2±*3427.97* $\bar{i}$	−6.71E2±*5019.74* $\bar{i}$	−6.86E2±*6382.81* $\bar{i}$	−7.00E2±*7437.27* $\bar{i}$
8.19	−9.74E2±*1488.53* $\bar{i}$	−9.87E2±*3348.52* $\bar{i}$	−1.01E3±*4963.69* $\bar{i}$	−1.03E3±*6336.74* $\bar{i}$	−1.05E3±*7396.10* $\bar{i}$
0.0	1.29E−8±*1778.23* $\bar{i}$	−3.35E−8±*3490.16* $\bar{i}$	2.52E−8±*5064.09* $\bar{i}$	−9.22E−8±*6419.41* $\bar{i}$	−1.01E−8±*7470.03* $\bar{i}$

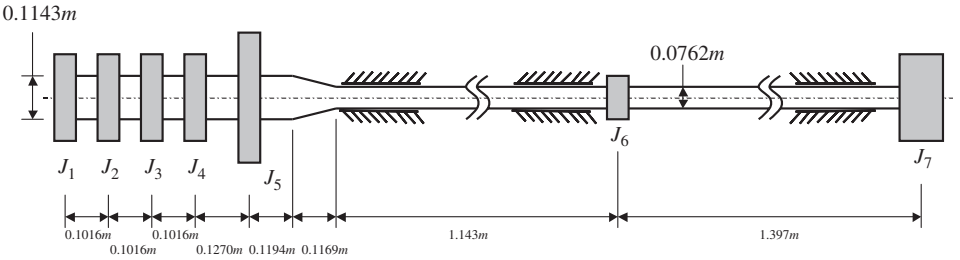

Fig. 5. Transmission shaft of a generator.

Table 5
The first five eigenvalues, $\bar{\omega}_j = \bar{\omega}_{jR} \pm \bar{i}\bar{\omega}_{jI}$ ($j = 1$ to 5), of a generator transmission shaft, as shown in Fig. 5, and the corresponding ones of the associated bare shaft

Systems	Eigenvalues, $\bar{\omega}_j = \bar{\omega}_{jR} \pm \bar{i}\bar{\omega}_{jI}$ ($j = 1$ to 5) (rad/s)				
	$\bar{\omega}_1$	$\bar{\omega}_2$	$\bar{\omega}_3$	$\bar{\omega}_4$	$\bar{\omega}_5$
Generator transmission shaft	−1.19E−9±*510.41* $\bar{i}$	1.65E−8±*2845.85* $\bar{i}$	−3.32E−8±*6211.09* $\bar{i}$	5.63E−8±*7617.05* $\bar{i}$	5.18E−9±*9320.98* $\bar{i}$
Bare shaft[a]	−1.39E−8±*2420.46* $\bar{i}$	−7.65E−8±*5964.36* $\bar{i}$	5.23E−9±*9705.35* $\bar{i}$	−1.03E−7±*13392.74* $\bar{i}$	7.47−8±*16319.06* $\bar{i}$

[a]The bare shaft refers to the shaft without carrying any disks.

smaller than that on the decay ratios, $\bar{\omega}_{jR}$ (i.e., the real parts of the eigenvalues). For this reason, the damping coefficients will have significant influence on the forced vibration responses of the shafting system.

6.4. Eigenvalues of a hybrid (tapered) shaft carrying three disks

To show applicability of the presented tapered shaft element for an engineering problem, a generator transmission shaft as shown in Fig. 5, is investigated in this subsection. The given data for the current shaft are: shear modulus $G = 8.01 \times 10^{10}\,\mathrm{N/m^2}$, mass density $\rho_s = 7820\,\mathrm{kg/m^3}$, and mass moments of inertia of the disks $J_1 = J_2 = J_3 = J_4 = 0.0308\,\mathrm{kg\,m^2}$, $J_5 = 1.4322\,\mathrm{kg\,m^2}$, $J_6 = 0.0279\,\mathrm{kg\,m^2}$, $J_7 = 0.4895\,\mathrm{kg\,m^2}$. Table 5 shows the first five eigenvalues of transmission shaft, $\bar{\omega}_j = \bar{\omega}_{jR} \pm \bar{i}\bar{\omega}_{jI}$ ($j = 1$ to 5). From the table, it can be seen that attachment of disks to the transmission shaft significantly influences the eigenvalues of the shafting system.

7. Conclusions

This paper presents a new *tapered shaft element* such that the torsional vibration characteristics of a damped shafting system can be easily determined with the continuous non-uniformity of cross-sections of the shaft being considered. The presented technique can be applied to the torsional vibration analysis of a hybrid shaft (i.e., a shaft composed of multiple *uniform* and *tapered* shaft segments) carrying multiple disks. Based on the presented numerical results and discussions, it has been found that the non-uniformity of cross-sections of the tapered shaft, and the damping coefficients have significant influences on the vibration characteristics of a shafting system.

References

[1] Y.Z. Chen, Torsional free vibration of a cylinder with varying cross-section and adhesive masses, *Journal of Sound and Vibration* 241 (3) (2001) 503–512.
[2] M. Aleyaasin, M. Ebrahimi, R. Whalley, Multivariable hybrid models for rotor-bearing systems, *Journal of Sound and Vibration* 233 (2000) 835–856.
[3] K. Koser, F. Pasin, Torsional vibrations of the drive shafts of mechanisms, *Journal of Sound and Vibration* 199 (1997) 559–565.
[4] J.S. Wu, C.H. Chen, Torsional vibration analysis of gear-branched systems by finite element method, *Journal of Sound and Vibration* 240 (2001) 159–182.
[5] Y.A. Khulief, M.A. Mohiuddin, On the dynamic analysis of rotors using modal reduction, *Finite Elements in Analysis and Design* 26 (1997) 41–55.
[6] H.Q. Qing, X.M. Cheng, Coupled torsional-flexural vibration of shaft systems in mechanical engineering—I. Finite Element Model, *Computers & Structures* 58 (1996) 835–843.
[7] H.D. Nelson, J.M. Mcvaugh, The dynamics of rotor-bearing systems using finite elements, *Journal of Engineering for Industry* 98 (1976) 593–600.
[8] E.S. Zorzi, H.D. Nelson, Finite element simulation of rotor-bearing systems with internal damping, *Journal of Engineering for Power* 99 (A1) (1977) 71–76.
[9] J.S. Wu, I.H. Yang, Computer method for torsion-and-flexure-coupled forced vibration of shafting system with damping, *Journal of Sound and Vibration* 180 (3) (1995) 417–435.
[10] B.O. Al-Bedoor, Transient torsional and lateral vibrations of unbalanced rotors with rotor-to-stator rubbing, *Journal of Sound and Vibration* 229 (2000) 627–645.
[11] M.A. Mohiuddin, Y.A. Khulief, Modal characteristics of rotors using a conical shaft finite element, *Computer Methods in Applied Mechanics and Engineering* 115 (1994) 125–144.
[12] R.C. Hibbeler, *Mechanics of Materials*, Prentice-Hall, Englewood Cliffs, NJ, 2004.
[13] R.W. Clough, J. Penzien, *Dynamics of Structures*, McGraw-Hill, New York, 1993.
[14] K.J. Bathe, *Finite Element Procedures in Engineering Analysis*, Prentice-Hall, Englewood Cliffs, NJ, 1982.
[15] L. Meirovitch, Analytical Methods in Vibrations. Macmillan Company, London, 1967.
[16] B.S. Garbow, *Matrix Eigensystem Routine—EISPACK Guide Extension*, Springer, Berlin, 1977.
[17] J.S. Przemieniecki, *Theory of matrix structural analysis*, McGraw-Hill, New York, 1985.